Original Article

JOURNAL OF THERMOPLASTIC COMPOSITE MATERIALS

Journal of Thermoplastic Composite Materials
2025, Vol. 38(9) 3437–3455

DOI: 10.1177/08927057251314411
journals.sagepub.com/home/jtc
Sage

Processing of reactive acrylic thermoplastic resin at elevated temperatures for rapid composite and fiber metal laminate manufacturing

Moritz Kruse[1], Maria Balk[2], Axel T Neffe[2,*] and Noomane Ben Khalifa[1,3]

Abstract

Thermoplastic polymers are increasingly being used as matrix materials for composites because they offer the advantage of recyclability and joinability over thermoset matrix systems. The polymerization kinetics and gas formation of different precursor mixtures of the liquid acrylic matrix system Elium® were investigated with different initiator contents and at different temperatures for accelerated processing of composites and fiber metal laminates. The mechanical and thermal properties of the resulting polymers showed no significant difference between the investigated parameters. However, the polymerization time was successfully reduced to under 15 minutes with higher temperatures and initiator contents in laminates with 1 mm thickness. In bulk polymerization and thicker laminates, the right parameters must be chosen to balance polymerization time and matrix heating to avoid gas formation leading to voids in the matrix. A combination of 75 wt% Elium® 130 and 25 wt% Elium® 190 with 1.25 wt% peroxide initiator at 50 °C was found to be

[1]Institute for Production Technology and Systems, Leuphana University of Lüneburg, Lüneburg, Germany
[2]Institute of Functional Materials for Sustainability, Helmholtz-Zentrum Hereon, Teltow, Germany
[3]Institute of Materials and Process Design, Helmholtz-Zentrum Hereon, Geesthacht, Germany

*BTU Cottbus-Senftenberg, Institute of Materials Chemistry, Senftenberg, Germany.

Corresponding authors:
Moritz Kruse, Institute for Production Technology and Systems, Leuphana University of Lüneburg, Universitätsallee 1, 21335 Lüneburg, Germany.
Email: moritz.kruse@leuphana.de

Maria Balk, Institute of Functional Materials for Sustainability, Helmholtz-Zentrum Hereon, Kantstraße 55, 14513 Teltow, Germany.
Email: maria.balk@hereon.de

optimal for reducing gas formation while simultaneously accelerating the polymerization reaction in 3-5 mm thick layers.

Keywords
Polymethylmethacrylate, polymerization kinetics, thermoplastic composites, elium®, fiber metal laminates

Introduction

Polymers and composite materials are increasingly applied in different sectors such as transportation to reduce weight and emissions. Composite materials aim at combining beneficial properties of two or more material classes and require special processing techniques as well as control over the interface of the materials. Fiber metal laminates (FML) were introduced in the aerospace industry to improve the impact resistance of fiber-reinforced polymers (FRP) while maintaining the advantage of high specific strength.[1] FMLs consist of several layers of metal and FRP, with the matrix of the FRP ensuring bonding at the interface between the two materials. This material combination offers the advantages of both materials, resulting in a high specific strength, exceptional fatigue resistance, impact tolerance, and corrosion resistance for high-performance applications.[2] Traditionally, these materials have been manufactured in an autoclave, using pre-impregnated fabric materials with a thermoset matrix. However, while simple curved structures, as required that is for aircraft fuselage structures, can be manufactured by this process, more complex geometries as necessary for many other applications cannot be manufactured because of insufficient pressure of the autoclave for forming. Furthermore, the resulting FML parts have very low formability in traditional metal forming processes, such as stamp forming or deep drawing, due to the cured matrix and the lack of plastic deformability of the fibers.[3] Hence, FMLs are rarely used for small parts with sharp curvatures. To improve the formability of FMLs in these processes, the application of semi-cured[4,5] and thermoplastic[6,7] materials in the FRP layer have been investigated. However, failure modes such as delamination, matrix accumulations as well as metal or fiber wrinkling and tearing can still occur,[8] depending on the process parameters and favored by the high matrix viscosity of the semi-cured and thermoplastic materials.[9]

To avoid these failure modes and improve the formability by reducing the fluid-structure interaction during the deep drawing, the previously developed in situ hybridization process utilizes a low viscous resin precursor.[9,10] Instead of using pre-impregnated fabric material, dry glass fiber fabrics are used in between two metal sheets (Figure 1). Two process routes are possible. The resin precursor can be applied by hand on top of the fabric layers before placing the top metal layer (wet compression molding – WCM). Alternatively, the low viscous resin precursor can be injected through a channel in the punch and a hole in the bottom metal sheet into the fabric layer during deep

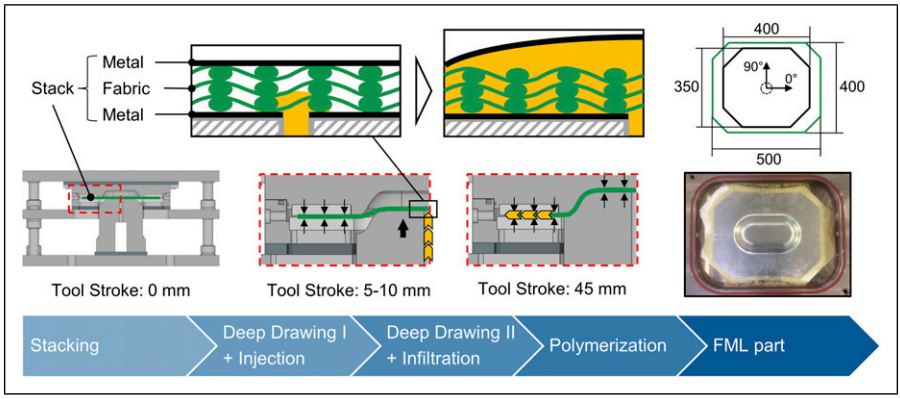

Figure 1. In situ hybridization: Combined deep drawing and resin transfer molding process (adapted from[10,11]).

drawing (resin transfer molding – RTM). Bulging of the upper metal sheet can occur due to the injection pressure and strong fabric compaction in the flange which reduces the polymer flow. Towards the end of the deep drawing process, the bulge is compressed between punch and die, reducing the matrix accumulation in the center and distributing it radially. After forming, the part is continuously compressed until the matrix is fully polymerized.

For this process, a reactive, low viscous (0.1 Pas), thermoplastic resin precursor (Arkema Elium® 150) has been used. Thermoplastic matrices offer the benefits of recyclability and joinability over thermoset systems.[11,12] However, early-generation reactive thermoplastic systems such as polybutylene terephthalate (PBT), polyamide-6 (PA-6), and polyamide-12 (PA-12) require high mold temperatures above 150 °C.[13] Elium® is the first thermoplastic matrix system suitable for reactive polymerization at low temperatures, therefore broadening the possible applications, that is for large structures where mold heating is difficult. It consists of a high content of methyl methacrylate (MMA) monomers. By using a radical initiator, MMA is converted into poly (methyl methacrylate) (PMMA) in free-radical polymerization, even at room temperature.[14,15] Several investigations into the mechanical properties of composites manufactured with Elium® have been carried out previously[16,17] and have shown that continuous glass fiber-reinforced polymers manufactured with Elium® exhibit similar mechanical properties to those manufactured with traditional epoxy systems.[13] In fiber metal laminates, the matrix-metal interface also strongly influences the overall mechanical performance. Therefore, several investigations have been conducted to improve the bonding strength, showing that various surface treatments of the metal can enhance the interlaminar shear strength of the fiber metal laminates. Mamalis et al.[18] have investigated various chemical, electrochemical and plasma treatments for Elium® based FML and achieved improved adhesion with all treatments studied. Shanmugam et al.[19] investigated two electrochemical treatments, anodization and micro-arc oxidation, and showed that micro-arc oxidation treatment significantly

improved the interlaminar shear strength of titanium-based fibre metal laminates compared to multi-step anodization. They later showed that a combination of anodising with subsequent etching and annealing increases the interlaminar fracture toughness by approximately 500 %.[20]

However, only very few investigations have been carried out regarding the polymerization kinetics of Elium® and how it can be influenced. The low viscosity of Elium® at room temperature allows for the easy impregnation of fabric materials, making it suitable for various RTM/VARTM processes and in situ hybridization. For the in situ hybridization process, a low viscosity during the forming process and fast polymerization after forming are advantageous to achieve good part quality and short process times. The polymerization time can be modified by the temperature, initiator content, and the Elium® mixture. The applied Elium® 150 contains a mixture of a slow reactive (Elium® 130) and fast reactive component (Elium® 190). Raponi et al.[21,22] previously investigated the influence of Luperox® 78 initiator content and thermal cycles on the polymerization kinetics. Pantelelis[23] developed an advanced microwave and cure monitoring system to accelerate the reaction at higher temperatures. However, the accelerated polymerization can lead to high internal temperatures due to a strong exothermic reaction, particularly in regions with matrix accumulations.[24] When peak temperatures exceed the boiling point of the resin at approximately 100 °C, gas formation and voids in the finished product can be generated, as shown by Murray et al.[25] and Han et al.[26] The presence of voids strongly decreases the mechanical properties of the fiber-reinforced polymers.[27] Han et al.[26] investigated the overheating of the Elium® resin during polymerization and proposed a thermo-chemical process model to predict temperature evolution and degree of polymerization. They also found that heat development was stronger with increased layer thickness of a fiber-reinforced polymer. Similarly to thermoset resins, high temperatures during Elium® polymerization can also lead to unwanted residual stresses and shape distortions due to thermal gradients.[28] On the other hand, higher polymerization temperatures resulted in higher interlaminar shear strength of a composite compared to polymerization at room temperature.[29]

The reactive acrylic thermoplastic matrix system Elium® offers a viable alternative to conventional thermoset systems for the in situ hybridization process. However, the highly exothermic reaction and overheating during polymerization, in particular in matrix accumulations as occurring during forming, influence the selection of suitable process parameters. This study aims to investigate the polymerization kinetics of different Elium® 130 (E130) to Elium® 190 (E190) ratios with different initiator contents at different temperatures to determine a parameter set for fast processing while minimizing void content. The polymerization kinetics were investigated by qualitative manual experiments and by shear oscillation measurements. In addition, characterizations of the resulting molar masses of PMMA copolymers, thermal transitions, and thermo-mechanical properties are conducted. Demonstrating parts are then produced via the in situ hybridization process with different parameter sets to validate the findings for composite and fiber metal laminate processing.

Material and experimental methods

Material

The acrylic resin precursor mixtures Elium® 190 (slow polymerizing) and Elium® 130 (fast polymerizing) from Arkema (Colombes, France) with an initial viscosity of 0.1 Pa•s at room temperature were investigated. Perkadox® GB-50X powder (Nouryon Specialty Chemicals, Amsterdam, Netherlands) containing 50 wt% dibenzoyl peroxide was used as the radical polymerization initiator. Two DC04 (1.0338) steel sheets and six plies of twill-woven E-glass fabric (280 g/m^2, Interglas 92,125 FE800, Eclose-Badinières, France) were used for the in situ hybridization experiments. A 0.025 mm thick PTFE foil (High-Tech-Flon, Konstanz, Germany) was placed between the tool and the top blank for lubrication.

Void formation

Thin layers of Elium® were polymerized in a cup with different parameter variations to qualitatively investigate the influence of different parameters on void formation and polymerization time and to define parameter sets for the analysis of molar masses, thermal and mechanical properties, and for kinetic investigations. An overview of the parameters investigated is given in Table 1. Samples were prepared in a paper cup by mixing the Elium® precursor mixtures and initiator by hand for approximately 1 minute and then placed in a convection oven. Void formation and viscosity were evaluated qualitatively every 5 minutes.

Rheological measurements

Twenty parameter combinations were selected for further investigation. Rheological measurements were carried out at 50 °C and 70 °C for each combination with E130 content from 0 wt% to 100 wt% and initiator content of 1.25 wt% and 2.5 wt%. The temperatures were selected based on the results of the void formation experiments which show that at 30 °C the polymerization time is too long for fast composite processing and that at 90 °C very strong void formation is observed. The kinetics of the polymerization reaction were investigated by oscillatory rheological experiments using a Haake Rheowin Mars II (Thermo Scientific, Karlsruhe, Germany) with a cone-plate geometry (diameter of

Table 1. Investigated parameters.

Parameter	Values
E130 content	0 %; 25 %; 50 %; 75 %; 100 %
Temperature	30 °C; 50 °C; 70 °C; 90 °C
Initiator content	1.25 wt%; 2.5 wt%
Layer thickness	3 mm; 5 mm

cone = 25 mm) with heated plate. The applied frequency and amplitude were kept low (f = 1 Hz, γ = 0.1 %) to minimize external influence on the measurement. To the mixtures of E130 and E190, the initiator was added at a defined concentration, the reaction mixture was stirred for 10 s at 22 °C and the reaction mixture was transferred to the rheometer. Measurements were started immediately and carried out with a cone-plate distance of 0.05 mm.

Gel permeation chromatography

The synthesis was performed for 24 h to ensure a complete polymerization process. GPC measurements were performed at a solvent flow rate of 1 mL·min^{-1} at 35 °C using chloroform as eluent and 0.2 wt% toluene as internal standard. The system was equipped with a pre-column, two 300 mm × 8.0 mm linear M columns (Polymer Standards Service GmbH (PSS), Mainz, Germany), an isocratic pump 2080, an automatic injector AS 2050 (both Jasco, Tokyo, Japan), a refractive index detector (Shodex RI-101, USA), and a differential viscometer/light scattering dual detector T60 A (Viscotek Corporation, Houston, USA). The SEC software WINGPC 6.2 (PSS) was used to determine the molar mass distributions by universal calibration with polystyrene standards (PSS).

Differential scanning calorimetry

Thermal properties of the polymerized specimens were determined on a Netzsch DSC 204 (Netzsch Ltd, Selb, Germany) in sealed Al-pans under N_2-atmosphere between −100 °C and 150 °C with heating and cooling rates of 10 K·min^{-1}. Sample masses ranged from 5.07 g to 6.66 g and the glass transition temperatures (T_gs) were determined from the second heating run.

Tensile tests

Films of the polymers after complete polymerization with thicknesses of (0.3 ± 0.1) mm were prepared using a Collin compression molding machine (Dr Collin GmbH, Ebersberg, Germany). The raw product was covered with PEEK film between two stainless steel plates and melted at 150 °C. A pressure of 100 bar was applied for 5 min to form the 2D films and then held constant during cooling of the compression molded specimens. Tensile tests (standard test specimens ISO 527-2/1BB) were performed at 25 °C and the tensile tester (Zwick Z1.0, Ulm, Germany) was equipped with a thermal chamber and a temperature controller (Eurotherm Regler, Limburg, Germany). A strain rate of 5 mm·min^{-1} was used.

In situ hybridized parts

Two fiber metal laminate parts were manufactured with the in situ hybridization process, as described in the introduction, under different polymerization conditions, to investigate the void formation in the glass fiber-reinforced polymer (GFRP) layer. The blank

holder force was 120 kN. Injection was performed at a drawing depth of 15 % of the total drawing depth of 45 mm for 60 s at an injection pressure of 8 bar. The deep drawing velocity was 1 mm/s until 38 mm drawing depth and 0.2 mm/s for the last 7 mm deep drawing to reduce the fluid-structure interaction. A release agent (Henkel Loctite® Frekote HMT2) was applied between the metal sheet and the GFRP layer so that the metal sheets could be removed after the process to investigate the GFRP layer separately. The release agent has previously been shown to have no effect on the forming process.[30] From the void formation experiments, 70 °C, 50 % E130, and 2.5 % initiator as well as 50 °C, 75 % E130, and 1.25 % initiator were selected as polymerization conditions.

Results and discussion

In the following section, samples are referenced according to the following scheme:
E(*E130 content in %*)P(*Initiator content in wt%*)$_{\mathrm{T\ Temperature\ in\ °C}}$

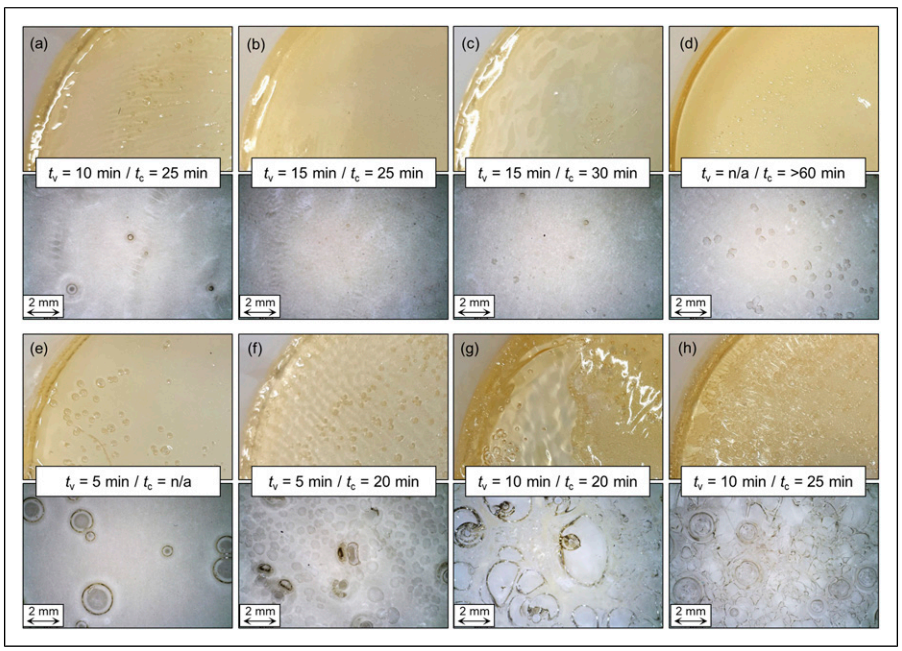

Figure 2. Macroscopic and mesoscopic images of the voids in Elium® samples (E130 content: (a)/(e) 100 wt%; (b)/(f) 75 wt%; (c)/(g) 50 wt%; (d)/(h) 25 wt%) with 3 mm thickness and 2.5 wt% initiator polymerized at (a)-(d) 50 °C and (e)-(h) 70 °C. The time until void formation was first observed t_v and the polymerization time t_c are given.

Void formation

Figure 2 shows the influence of Elium® precursor mixture and temperature on void formation and polymerization time. Higher temperatures increase polymerization speed and reduce the polymerization time. However, strong void formation is observed at polymerization temperatures of 70 °C and above, which could be related to a rapid temperature increase above the boiling temperature of 100 °C. Void size also appears to be temperature dependent, with higher temperatures resulting in larger voids, possibly because the resin reaches the boiling temperature at lower degrees of polymerization. Thus, the viscosity during gas formation is lower, allowing the gas to coalesce and form larger voids. Han et al.[26] showed that at higher degrees of polymerization than 0.62, no void formation occurs even when the temperature rises above the resin's boiling point. At 50 °C, only a small amount of voids is observed depending on the Elium® precursor mixture, and no voids are observed when the polymerization is performed at 30 °C. As the time of complete curing at 30 °C is more than 50 minutes for all precursor mixtures, higher temperatures are required for shorter cycle times in the in situ hybridization process. The same is true for pure E190 at all temperatures which requires high temperatures or long reaction times. On the other hand, pure E130 does not fully polymerize at 70 °C, indicating a glass transition point below or around 70 °C. Interestingly, a higher content of the fast reacting E130 seems to simultaneously reduce polymerization times and gas formation during polymerization. As the exact composition of E130 and E190 is a company secret, it is unclear whether specific components in the E190 could facilitate void formation. Therefore, a precursor mixture of 75 wt% E130 and 25 wt% E190 polymerized at 50 °C appears to be optimal for fast polymerization with minimal void formation.

With lower initiator content, void formation is further reduced, but the time to complete curing is increased due to the reduced amount of free radicals generated to propagate the polymerization (Figure 3). It should be noted that the decomposition of

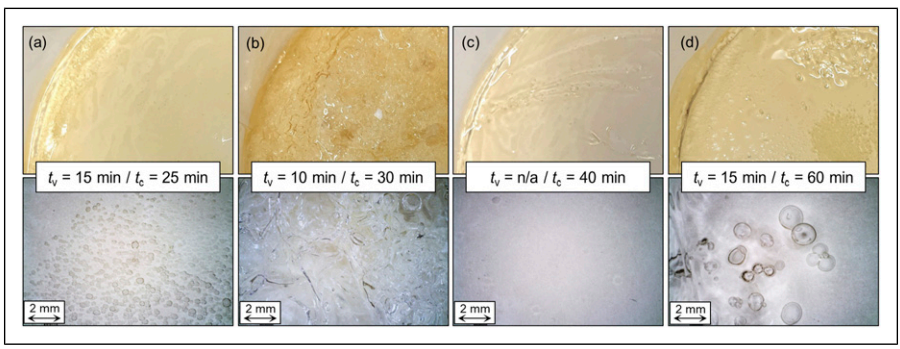

Figure 3. Macroscopic and mesoscopic images of the voids in Elium® samples with 75 % E130 polymerized at 50 °C: (a) 2.5 % initiator, 3 mm thick; (b) 2.5 % initiator, 5 mm thick; (c) 1.25 % initiator, 3 mm thick; (d) 1.25 % initiator, 5 mm thick. The time until void formation was first observed t_v and the polymerization time t_c are given.

the initiator (to generate the required free radicals) also leads to gas formation (release of CO_2). Hence, reducing the initiator content will reduce the amount of CO_2 produced. The layer thickness has a strong influence on void formation. With 2.5 wt% initiator in a 3 mm thick layer, only a few small voids were formed (Figure 3(a)), whereas in a 5 mm thick layer strong gas formation was observed (Figure 3(b)), leading to a foamy structure of the fully polymerized material. At 1.25 wt% initiator content, the effect is slightly less pronounced. In addition, thicker layers take longer to fully polymerization but void formation is observed earlier.

Polymerization process

Polymerization kinetics were investigated in detail using shear oscillation experiments to obtain the viscosity versus time for different polymerization conditions. Two dynamic viscosity curves as a function of time are shown in Figure 4, one for a fast polymerizing sample and one for a slow polymerizing sample.

During the initial induction period, the samples maintained their initial viscosity. The length of the initial plateau depended on the polymerization conditions and was very short for samples polymerized at 70 °C. For samples polymerized at 70 °C, a rapid increase in

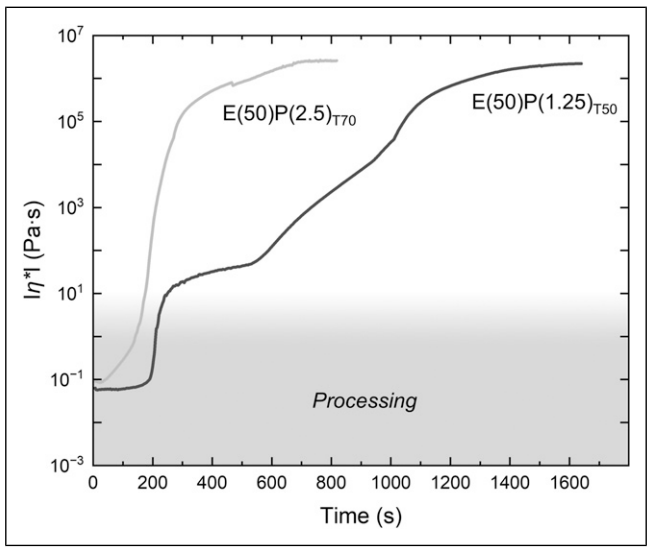

Figure 4. Dynamic viscosity ($|\eta^*|$) as a function of time for one fast and one slow polymerizing Elium® sample.

viscosity was observed until a plateau was reached when the sample was fully polymerized. For the slower reacting samples at 50 °C, another plateau is present between 10 and 100 Pa•s before the viscosity increases again until the sample is fully polymerized. During PMMA polymerization, strong gel, glass, and cage effects are present,[31,32] which affect the viscosity. For composite processing, the processing time, which determines how long fabric infiltration is possible, and the polymerization time, when the final part can be demolded, are relevant. To compare the influence of the initiator content, temperature, and Elium® precursor mixture, 1 Pa•s was chosen as the maximum processing viscosity, as higher viscosities can lead to high fluid forces and fabric defects during processing.[9] The time to reach 10^4 Pa•s is compared as a measure of polymerization times (Figure 5).

No polymerization time was obtained for pure E190 and E(25)P(1.25)$_{T50}$, because full polymerization took longer than 1000 s and was therefore not considered applicable for rapid composite processing. Both processing and polymerization times are primarily dependent on temperature, as the decomposition of the initiator is temperature dependent and the mobility of the monomers and chains increases with higher temperatures. At 70 °C, no effect of initiator content and Elium® mixture on the polymerization time was observed. At 50 °C, polymerization can be accelerated with higher initiator contents. Only at 50 °C and 1.25 wt% initiator content, an influence of the E130 content was be observed, where a higher E130 content led to a faster polymerization. However, no clear influence of the E130 content on the processing time was observed for any sample, whereas a higher initiator content increased the processing time, contrary to the influence on the polymerization time. While higher initiator contents initially lead to more free radicals in the system, they also lead to shorter chain lengths after complete polymerization. As these two effects compete with each other, higher initiator contents can result in longer processing times with simultaneously shorter polymerization times.

In composite processing, there is no isothermal reaction as the resin is not preheated but heated after injection into the mold. Due to thicker layers than in oscillatory rheology, slower heating of the resin results in slower polymerization, especially at the beginning of

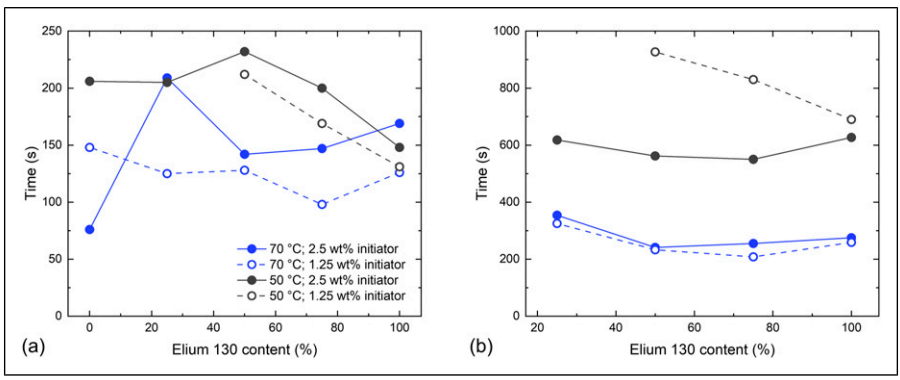

Figure 5. (a) Processing times (maximum 1 Pa•s) and (b) polymerization times (10^4 Pa•s was reached) for different E130 contents, initiator contents, and temperatures during polymerization.

the process, and therefore longer processing and polymerization times. Ignoring void formation, an initiator content of 2.5 wt%, E130 content of 50-100 wt%, and a mold temperature of 70 °C should be optimal for composite processing, as the processing time would probably be closer to 200-250 s due to the initial resin heating while the polymerization time is minimized.

Investigation of material characteristics

The Elium® samples were analyzed after complete polymerization by GPC measurements to investigate the generated molar masses of the PMMA, as the polymer chain length affects material characteristics such as thermal and mechanical properties.[33,34] As presented in Figure 6, the molar masses were influenced by the E130 to E190 content. A decrease in the number average molar mass M_n from (85 ± 9) kg·mol^{-1} for samples consisting of 0 wt% E130 and 100 wt% E190 to (49 ± 9) kg·mol^{-1} for Elium® samples based on 100 wt% E130 was detected. Since E130 is the fast polymerizing component with increased kinetics as determined by shear oscillation measurements, the growth of polymer chains is faster compared to mixtures with a high amount of E190. As the diffusion of the monomers (MMA) is time-dependent and is hindered by the increasing viscosity over time during polymerization, the resulting lower M_n could be attributed to

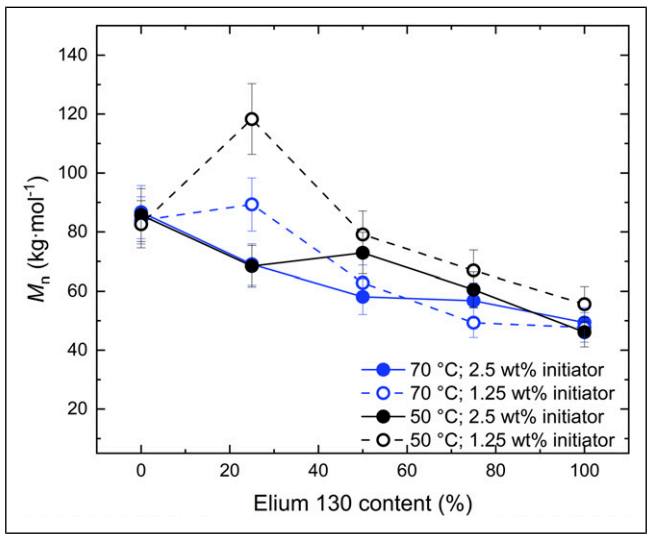

Figure 6. Number average molar mass M_n of Elium® samples as a function of the E130 content.

reduced monomer accessibility. As a second parameter, the reaction temperature, which was applied during the radical polymerization, also influences the resulting PMMA chain length. When the polymerization is performed at 50 °C, higher M_n values are created. In this case, the reaction kinetics are slower compared to the process at 70 °C, which facilitates the diffusion of unreacted monomers during polymerization. The content of dibenzoyl peroxide as initiator presents a third parameter affecting the molar masses. Here, the PMMA chain length is higher when a low initiator content of 1.25 wt% is used. The decomposition of the dibenzoyl peroxide generates radicals that are required to initiate the polymerization process. The lower the amount of radicals created, the lower the number of growing chains. If the amount of monomers is kept constant, higher M_ns can be achieved. It should be noted that the obtained dispersity of molar masses is high, ranging from 1.8 to 4.5, without a significant influence of the temperature, E130 content, or initiator content. However, since this type of reaction is not a controlled radical polymerization, such high dispersity values are not unusual.

The thermal properties of the resulting Elium® samples were analyzed by DSC measurements from the second heating run. As shown in Figure 7, T_g values ranging from 73 °C to 110 °C were observed. No clear influence of the reaction temperature, E130 content, or of the wt% of the initiator (which affects the molar masses) on T_g could be observed. As described in the literature, when M_n of PMMA is higher than

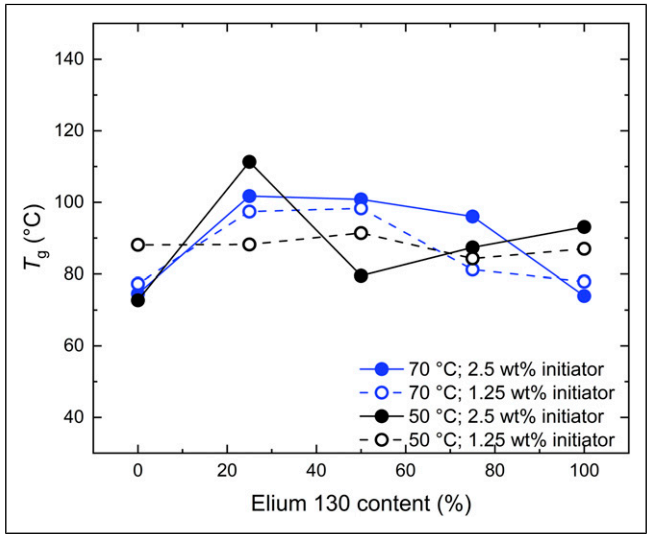

Figure 7. Thermal properties of Elium® samples as a function of the E130 content.

30 kg·mol^{-1}, no significant changes in the thermal properties could be detected, with a maximum T_g of about 135 °C.[35] Since the obtained Elium® samples provided M_n values higher than (49 ± 9) kg·mol^{-1}, the T_g is independent of the synthesis variations. The determined thermal properties of Elium® samples are lower than the described maximum, which could be attributed to the presence of unreacted MMA monomers. To enable the transfer of these experiments to the in situ hybridization process, the reaction mixture was not stirred during radical polymerization and the samples were not extracted after polymerization. Therefore, the MMA could act as a softening agent resulting in lower T_g values.

Tensile tests of Elium® samples (Figure 8) were performed to investigate the mechanical properties as a function of the E130 content, polymerization temperature, and initiator content. As shown in Figure 8(b), the E-moduli ranged from 1300 MPa to 2100 MPa and were within the margin of error. Similar to the discussion of the thermal properties, an influence of the Elium® ratio, polymerization temperature, and initiator content on the resulting E values could not be detected because the molar masses of the synthesized PMMAs are high and an increase in the polymer chain length no longer affects the material properties. Furthermore, the uncontrolled radical polymerization

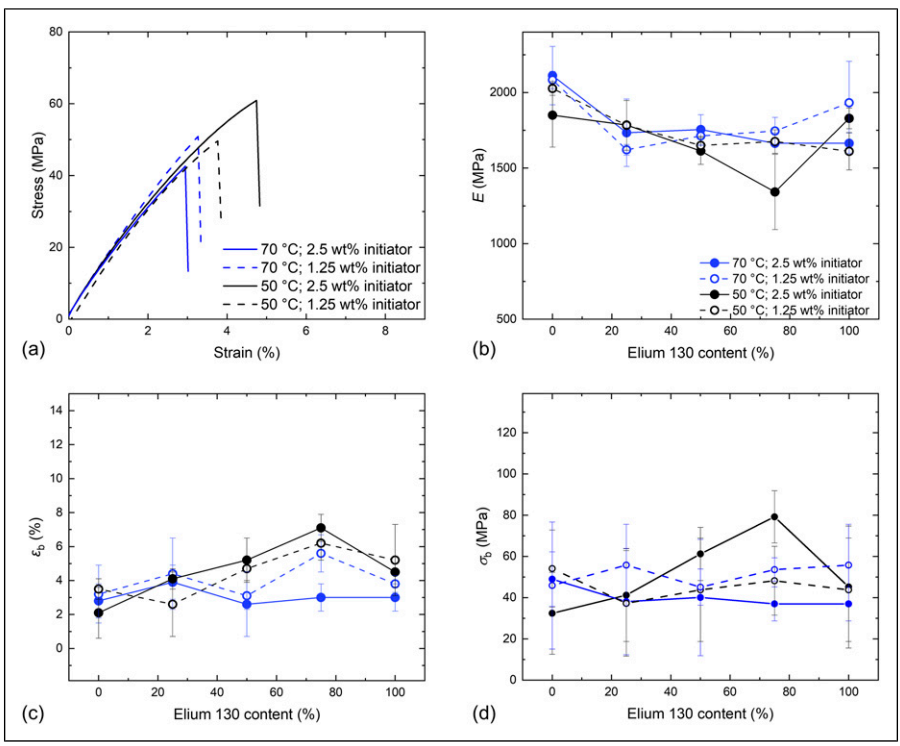

Figure 8. Tensile properties of Elium® samples: (a) Exemplary stress-strain curves with 50 % E130; (b) *E*-modulus, (c) elongation at break and (d) tensile strength as a function of the E130 content.

results in large deviations in mechanical properties for all parameter combinations investigated. The E-moduli obtained are lower than those reported in the literature (E = 3180 MPa[36]). Since the unreacted MMA was not extracted from the obtained PMMA films, unreacted monomers acting as a softening agent could reduce the E-modulus. In good agreement with the literature,[37] the synthesized PMMA exhibits a tensile strength between 30 MPa and 80 MPa (Figure 8(d)) and almost brittle fracture with a limited elongation at break (ε_b) between 2 % and 7 % at room temperature (Figure 8(c)), which was mostly independent of the E130 content, temperature used for polymerization, and initiator amount.

In composites, the primary function of the matrix is to align and stabilize the reinforcement fibers and to transfer load into the fibers. Thus, the interface bonding to the fabric material, which depends on the polymer-fabric sizing combination, is more relevant than the mechanical properties of the matrix material.[38] However, the mechanical properties of the matrix still influence the overall mechanical performance of the composite under certain loads, that is under transverse compression[39] and impact.[40] The measured elongations at break are in a similar range to the ductility of commonly used fiber materials (glass fiber 3-5 %; carbon fiber 1-2 %). It can be concluded that all the polymerization conditions investigated are adequate for the processing of composites in terms of the thermal and mechanical properties of the resulting matrix material, with only minor differences observed.

In Situ Hybridized Parts

Polymerization conditions for the in situ hybridized parts were selected based on the void formation experiments (Figure 2/Figure 3). With E(50)P(2.5)$_{T70}$, strong gas formation can be expected, while with E(75)P(1.25)$_{T50}$ no or very little gas formation was observed. As was shown in Figure 3(c) and (d), void formation was observed only after 15 min and in layers thicker than 3 mm with E(75)P(1.25)$_{T50}$. The glass fiber reinforced polymer

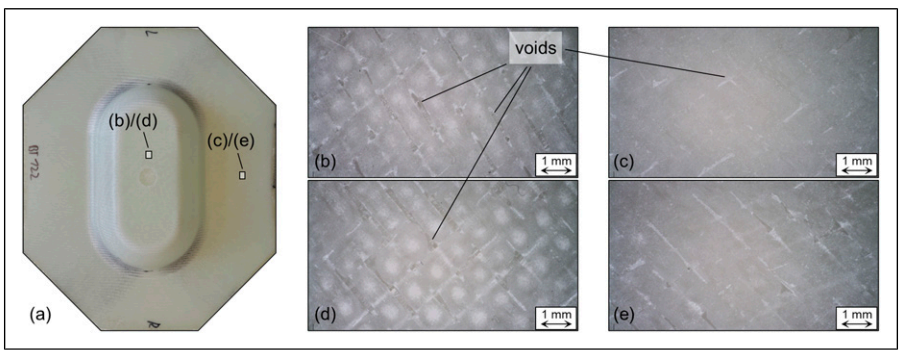

Figure 9. GFRP layer (1 mm thickness) of an in situ hybridized fiber metal laminate: (a) Location of microscopic images; (b) E(50)P(2.5)$_{T70}$, part bottom; (c) E(50)P(2.5)$_{T70}$, flange; (d) E(75)P(1.25)$_{T50}$, part bottom; (e) E(75)P(1.25)$_{T50}$, flange.

(GFRP) layer of the resulting part has a thickness of 1 mm and is shown in Figure 9. Since the forming of the GFRP part is completed approximately 3 min after mixing resin and initiator, gas formation due to matrix polymerization is very unlikely with $E(75)P(1.25)_{T50}$. However, meso voids were observed between the fiber rovings in both parts and in the part bottom as well as the flange. Furthermore, there was no difference in void formation in the GFRP layer between the two polymerization conditions, and even slightly fewer voids were present in the flange after polymerization at higher temperatures.

This indicates that the present voids are not caused by the matrix, but by the process itself. Therefore, application of the thermoplastic matrix precursors at elevated temperatures is feasible to accelerate polymerization without causing gas formation in thin GFRP parts. However, since the heat generation and void formation are also dependent on the layer thickness, further investigations are required for thicker laminates. Since no significant differences were found in the tensile properties of the different polymers, only small differences in the mechanical properties of the manufactured GFRP layers are expected to occur due to differences in void content. However, the differences are expected to be insignificant compared to the strong influence of the metal-matrix interface quality, which for the here used materials can be enhanced by grinding and applying a chemical bonding agent,[41] as well as the fiber orientation due to the fabric forming in the process. It was previously demonstrated for this geometry that the mechanical properties can vary considerably across different regions due to fiber draping.[42]

Conclusion

Various reactive acrylic thermoplastic resin precursor mixtures, specifically Elium® 130 (fast polymerizing) and Elium® 190 (slow polymerizing), were studied with respect to their polymerization kinetics at elevated temperatures, gas formation due to overheating, and the properties of the resulting polymer. While the molar masses of the polymers were dependent on the polymerization conditions, the reached M_ns $\geq$49 kg·mol^{-1} of all polymers did not result in significant differences in mechanical and thermal properties. The polymerization kinetics were highly dependent on temperature and initiator content, with a slight influence of the resin precursor mixture. Higher temperatures and initiator contents accelerated the polymerization reaction, reducing cycle times to less than 15 minutes for thin GFRP laminates. However, during bulk polymerization and presumably in thick GFRP laminates, overheating of the matrix led to gas formation and voids. Lower temperatures and initiator content, as well as different resin precursor mixtures, were successfully used to balance fast polymerization while avoiding void formation. A combination of 75 wt% E130 and 25 wt% E190 with 1.25 wt% peroxide initiator at 50 °C was found to be optimal for reducing gas formation while simultaneously accelerating the polymerization reaction in bulk polymerization of thicker matrix layers. As this may also depend on the fiber and matrix volume fraction of the manufactured GFRP, further investigations are required for the manufacturing of thick GFRP parts. In addition, while it was shown that there was no void formation due to matrix overheating in the manufactured fiber metal laminate parts, further investigation is needed to reduce air entrapment due to the in situ hybridization process itself.

Acknowledgements

The matrix precursor system and peroxide were kindly provided by the Arkema Group. The authors would like to thank N. Schneider, S. Schwanz and N. v. Stritzky for their help in performing the experiments.

Author Contribution

M.K. Conceptualization, Methodology, Formal analysis, Investigation, Data Curation, Writing - Original Draft, Visualization; M.B. Conceptualization, Methodology, Formal analysis, Investigation, Data Curation, Writing - Original Draft, Visualization; A.N. Conceptualization, Resources, Writing - Review & Editing, Project administration; N.B.K. Conceptualization, Resources, Writing - Review & Editing, Project administration, Funding acquisition.

Declaration of conflicting interests

The author(s) declared no potential conflicts of interest with respect to the research, authorship, and/or publication of this article.

Funding

The author(s) disclosed receipt of the following financial support for the research, authorship, and/or publication of this article: This work was supported by the German Research Foundation (DFG) [grant numbers BE 5196/4-1, BE 5196/4-2]. This work was supported by the Helmholtz Association through program-oriented funding.

ORCID iD

Moritz Kruse https://orcid.org/0000-0002-7716-579X

References

1. Vlot A. *Glare: history of the development of a new aircraft material*. Dordrecht: Kluwer Acad. Publ, 2001.
2. Etri HE, Korkmaz ME, Gupta MK, et al. A state-of-the-art review on mechanical characteristics of different fiber metal laminates for aerospace and structural applications. *Int J Adv Manuf Technol* 2022; 123: 2965–2991.
3. Blala H, Lang L, Sherkatghanad E, et al. An investigation into process parameters effect on the formability of GLARE materials using stamp forming. *Appl Compos Mater* 2019; 26: 1423–1436.
4. Blala H, Lang L, Khan S, et al. A comparative study on the GLARE stamp forming behavior using cured and non-cured preparation followed by hot-pressing. *Int J Adv Manuf Technol* 2021; 115: 1461–1473.
5. Heggemann T and Homberg W. Deep drawing of fiber metal laminates for automotive lightweight structures. *Compos Struct* 2019; 216: 53–57.
6. Zhao Z, Teng W, Zhang J, et al. Effect of forming temperature and fiber orientation on the warm deep drawing formability of TA2/Cf/PEEK laminates. *J Manuf Process* 2024; 116: 48–59.

7. Wollmann T, Hahn M, Wiedemann S, et al. Thermoplastic fibre metal laminates: stiffness properties and forming behaviour by means of deep drawing. *Arch Civ Mech Eng* 2018; 18: 442–450.
8. Ding Z, Wang H, Luo J, et al. A review on forming technologies of fibre metal laminates. *International Journal of Lightweight Materials and Manufacture* 2021; 4: 110–126.
9. Kruse M and Ben Khalifa N. Influencing parameters in the deep drawing of fiber metal laminates with low viscous matrix. In: Mocellin K, Bouchard P-O, Bigot R, et al. (eds). *Proceedings of the 14th International Conference on the Technology of Plasticity - Current Trends in the Technology of Plasticity*. Cham: Springer Nature Switzerland, 2024, pp. 124–134.
10. Mennecart T, Werner H, Ben Khalifa N, et al. Developments and analyses of alternative processes for the manufacturing of fiber metal laminates. In *Materials; joint MSEC-NAMRC-manufacturing USA*. NY, USA: American Society of Mechanical Engineers.
11. Werner HO, Poppe C, Henning F, et al. Material modeling in forming simulation of three-dimensional fiber-metal-laminates-A parametric study. In: 23rd International Conference on Material Forming (ESAFORM 2020), Cottbus, Germany, May 4-8, 2020, pp. 154–161.
12. Miranda Campos B, Bourbigot S, Fontaine G, et al. Thermoplastic matrix-based composites produced by resin transfer molding: a review. *Polym Compos* 2022; 43: 2485–2506.
13. Obande W, Ó Brádaigh CM and Ray D. Continuous fibre-reinforced thermoplastic acrylic-matrix composites prepared by liquid resin infusion – a review. *Compos B Eng* 2021; 215: 108771.
14. Bodaghi M, Park CH and Krawczak P. Reactive processing of acrylic-based thermoplastic composites: a mini-review. *Front Mater* 2022; 9.
15. Silveira DC, Braga TTS, Conejo LS, et al. Kinetic and viscoelastic study of liquid thermoplastic matrix based on methyl methacrylate copolymers. *Mat Res* 2023; 26.
16. Kazemi ME, Shanmugam L, Lu D, et al. Mechanical properties and failure modes of hybrid fiber reinforced polymer composites with a novel liquid thermoplastic resin, Elium®. *Compos Appl Sci Manuf* 2019; 125: 105523.
17. Barbosa LCM, Bortoluzzi DB and Ancelotti AC. Analysis of fracture toughness in mode II and fractographic study of composites based on Elium® 150 thermoplastic matrix. *Compos B Eng* 2019; 175: 107082.
18. Mamalis D, Obande W, Koutsos V, et al. Novel thermoplastic fibre-metal laminates manufactured by vacuum resin infusion: the effect of surface treatments on interfacial bonding. *Mater Des* 2019; 162: 331–344.
19. Shanmugam L, Kazemi ME and Yang J. Improved bonding strength between thermoplastic resin and Ti alloy with surface treatments by multi-step anodization and single-step micro-arc oxidation method: a comparative study. *ES Mater Manuf* 2019; 3: 57–65.
20. Shanmugam L, Kazemi ME, Rao Z, et al. On the metal thermoplastic composite interface of Ti alloy/UHMWPE-Elium® laminates. *Compos B Eng* 2020; 181: 107578.
21. de Andrade Raponi O, Righetti de Souza B, Miranda Barbosa LC, et al. Thermal, rheological, and dielectric analyses of the polymerization reaction of a liquid thermoplastic resin for infusion manufacturing of composite materials. *Polym Test* 2018; 71: 32–37.
22. Raponi OA, Barbosa LCM, de Souza BR, et al. Study of the influence of initiator content in the polymerization reaction of a thermoplastic liquid resin for advanced composite manufacturing. *Adv Polym Technol* 2018; 37: 3579–3587.

23. Pantelelis N, Bistekos E, Emmerich R, et al. Compression RTM of reactive thermoplastic composites using microwaves and cure monitoring. *Procedia CIRP* 2019; 85: 249–254.
24. Kruse M and Ben Khalifa N. Experimental investigation of the fluid-structure interaction during deep drawing of fiber metal laminates in the in-situ hybridization process. In: *Materials research proceedings*. Millersville, PA: Materials Research Forum LLC, pp. 977–986.
25. Murray RE, Penumadu D, Cousins D, et al. Manufacturing and flexural characterization of infusion-reacted thermoplastic wind turbine blade subcomponents. *Appl Compos Mater* 2019; 26: 945–961.
26. Han N, Baran I, Zanjani JSM, et al. Experimental and computational analysis of the polymerization overheating in thick glass/Elium® acrylic thermoplastic resin composites. *Compos B Eng* 2020; 202: 108430.
27. Mehdikhani M, Gorbatikh L, Verpoest I, et al. Voids in fiber-reinforced polymer composites: a review on their formation, characteristics, and effects on mechanical performance. *J Compos Mater* 2019; 53: 1579–1669.
28. Palmieri B, Petriccione A, De Tommaso G, et al. An efficient thermal cure profile for thick parts made by reactive processing of acrylic thermoplastic composites. *J Compos Sci* 2021; 5: 229.
29. Han N, Yuksel O, Zanjani JSM, et al. Experimental investigation of the interlaminar failure of glass/elium® thermoplastic composites manufactured with different processing temperatures. *Appl Compos Mater* 2022; 29: 1061–1082.
30. Kruse M, Lehmann J and Ben Khalifa N. Parameter investigation for the in-situ hybridization process by deep drawing of dry fiber-metal-laminates. In: Liewald M, Verl A, Bauernhansl T, et al. (eds). *Production at the Leading Edge of Technology*. Cham: Springer International Publishing, 2023, pp. 122–130.
31. Louie BM, Carratt GM and Soong DS. Modeling the free radical solution and bulk polymerization of methyl methacrylate. *J Appl Polym Sci* 1985; 30: 3985–4012.
32. Biondi M, Borzacchiello A and Netti PA. Isothermal and non-isothermal polymerization of methyl methacrylate in presence of multiple initiators. *Chem Eng J* 2010; 162: 776–786.
33. Ali U, Karim KJBA and Buang NA. A review of the properties and applications of poly (methyl methacrylate) (PMMA). *Polym Rev* 2015; 55: 678–705.
34. Wang H, Chang T, Li X, et al. Scaled down glass transition temperature in confined polymer nanofibers. *Nanoscale* 2016; 8: 14950–14955.
35. D'Amelia R P and Kreth E H. Establishment of the flory-fox equation for polymethyl methacrylate (PMMA) using differential scanning calorimetry (DSC) and determination of tacticity using quantitative proton nuclear magnetic resonance spectroscopy (qHNMR). *JPBPC* 2023; 11: 1–10.
36. Johnson JA and Jones DW. The mechanical properties of PMMA and its copolymers with ethyl methacrylate and butyl methacrylate. *J Mater Sci* 1994; 29: 870–876.
37. Abdel-Wahab AA, Ataya S and Silberschmidt VV. Temperature-dependent mechanical behaviour of PMMA: experimental analysis and modelling. *Polym Test* 2017; 58: 86–95.
38. Drzal LT and Madhukar M. Fibre-matrix adhesion and its relationship to composite mechanical properties. *J Mater Sci* 1993; 28: 569–610.
39. González C and Llorca J. Mechanical behavior of unidirectional fiber-reinforced polymers under transverse compression: microscopic mechanisms and modeling. *Compos Sci Technol* 2007; 67: 2795–2806.

40. Andrew JJ, Srinivasan SM, Arockiarajan A, et al. Parameters influencing the impact response of fiber-reinforced polymer matrix composite materials: a critical review. *Compos Struct* 2019; 224: 111007.
41. Werner H, Sönmez I, Wendel R, et al. Characterization of the interlaminar shear strength of fibre metal laminates with reactively processed thermoplastic matrix. In: SAMPE Europe Conference & Exhibition 2017 Stuttgart: Stuttgart, Germany, 14-16 November 2017.
42. Werner HO, Stern C and Weidenmann KA. Location-dependent mechanical properties of in situ polymerized three-dimensional fiber-metal laminates. *KEM* 2019; 809: 231–236.